May 2002 • NREL/CP-520-31440

Conference Paper

# A New Thin-Film $CuGaSe_2$/ $Cu(In,Ga)Se_2$ Bifacial, Tandem Solar Cell with Both Junctions Formed Simultaneously

## Preprint

D.L. Young, J. Abushama, R. Noufi, X. Li,
J. Keane, T.A. Gessert, J.S. Ward, M. Contreras
M. Symko-Davies, and T.J. Coutts

*To be presented at the 29th IEEE PV Specialists Conference*
*New Orleans, Louisiana*
*May 20-24, 2002*

**National Renewable Energy Laboratory**

**1617 Cole Boulevard**
**Golden, Colorado 80401-3393**

**NREL is a U.S. Department of Energy Laboratory**
**Operated by Midwest Research Institute • Battelle • Bechtel**

**Contract No. DE-AC36-99-GO10337**

# A NEW THIN-FILM $CuGaSe_2$ / $Cu(In,Ga)Se_2$ BIFACIAL, TANDEM SOLAR CELL WITH BOTH JUNCTIONS FORMED SIMULTANEOUSLY

David L. Young, Jehad Abushama, Rommel Noufi, Xiaonan Li, James Keane, Timothy A. Gessert, J. Scott Ward, Miguel Contreras, Martha Symko-Davies, and Timothy J. Coutts
National Renewable Energy Laboratory, 1617 Cole Blvd., Golden, CO 80401

## ABSTRACT

Thin films of $CuGaSe_2$ and $Cu(In,Ga)Se_2$ were evaporated by the 3-stage process onto opposite sides of a single piece of soda-lime glass, coated bifacially with an $n^+$-TCO. Junctions were formed simultaneously with each of the p-type absorbers by depositing thin films of n-CdS via chemical bath deposition (CBD) at 60˚C. The resulting four-terminal device is a non-mechanically stacked, two-junction tandem. The unique growth sequence protects the temperature-sensitive p/n junctions. The initial device ( = 3.7%, $V_{oc}$ = 1.1 V [AM1.5]) suffered from low quantum efficiencies. Initial results are also presented from experiments with variations in growth sequence and back reflectors.

## INTRODUCTION

The efficiency benefit of a tandem solar cell to that of a single-junction cell has long been recognized, but practically realized only in expensive crystalline III-V materials [1] or low-efficiency a-Si thin films [2]. Coutts *et al*. [3], modeling state-of-the-art, thin-film devices, identified optimum bandgaps for two-junction tandem thin-film solar cells. Their work showed that a current-matched, 28%-efficient tandem is possible with a top-cell absorber of 1.7 eV and a bottom-cell absorber of 1.1 eV. These bandgaps are ideally matched to the $CuInSe_2$ (0.95 eV) — $CuGaSe_2$ (1.7eV) material system. Single-junction $CuIn_xGa_{1-x}Se_2$/CdS solar cells [4] have achieved efficiencies greater than 18%, whereas $CuGaSe_2$/CdS cells [5] have reached efficiencies greater than 9% [6]. These record cells, however, are quite sensitive to temperatures above 200˚C, where diffusion destroys the p/n junction. This relatively low survival temperature for the individual cells has been identified as a show-stopper for many thin-film tandem devices because of the need to grow good-quality absorber materials at temperatures above 500˚C.

Figure 1 shows a traditional, monolithic, two-terminal tandem device structure with a substrate configuration. The bottom cell is grown first, with the high-temperature absorber layer grown before a low-temperature window layer. As is obvious from the diagram and our previous discussion, the shorting junction and the top cell must be grown at temperatures below about 200˚C so as not to destroy the already-completed bottom cell. In fact, a-Si tandem cells are limited somewhat in their device configuration due to the temperature-sensitive, B-doped p-layer. Most previously proposed polycrystalline tandem devices have either been coupled to single-crystal subcells [7] or mechanically stacked [8] to avoid the temperature limitations described above.

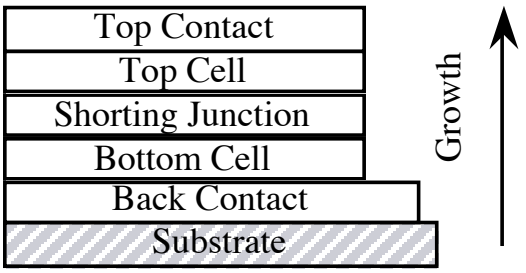

Figure 1. Traditional tandem.

In this paper, we propose a new device design that circumvents the temperature limitations of traditional monolithic tandem devices. Our design is a non-mechanically stacked, bifacial, four-terminal cell grown on a single substrate. Initial prototypes prove the concept to be viable, and ongoing experiments show improvements over our first attempts.

Our new device design is shown schematically in Fig. 2. The growth sequence for the device is also shown in Fig. 2 and starts (1) with transparent conducting oxide (TCO) layers deposited on each side of the glass substrate. Next (2), one of the p-type absorber

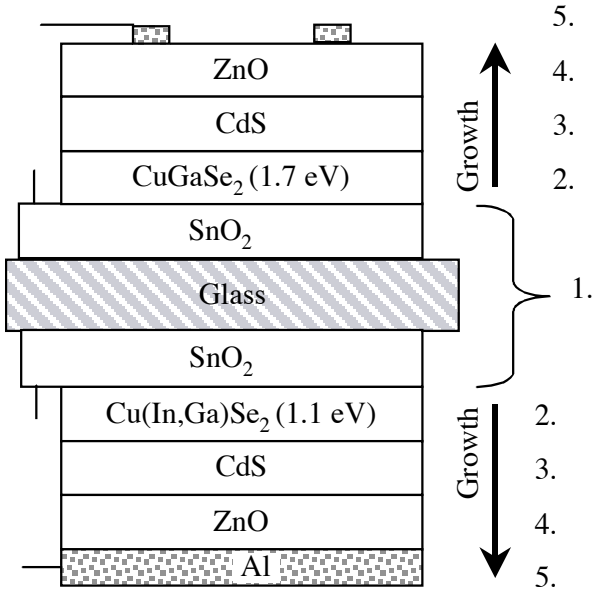

Figure 2. New tandem device.

layers is deposited at high temperature (>500 ˚C) onto one of the TCO layers. The substrate is then flipped over, and the other p-type absorber layer (2) is deposited onto the remaining TCO layer. The substrate is then dipped into a low-temperature (<100˚C) chemical bath, and n-CdS layers are grown (3) onto each of the absorber layers simultaneously. This step forms the p/n junctions for each cell in the tandem. Transparent (4) and metallic contacts (5) are grown next at room-temperature to complete the cells.

The growth sequence of the overall device ensures that once the p/n junctions are formed for both cells, the device is not exposed to further high temperatures that might destroy the electrical properties of the junctions. The choice as to which absorber is grown first in the above description depends on which absorber is more resilient to the temperature and growth atmosphere of the absorber grown second. It should be noted that if both absorber layers can be grown at the same temperature, then, theoretically, both layers could be grown simultaneously. The growth advantages inherent in this new tandem structure are somewhat offset by the less-than-ideal inverted bottom cell (light entering from the absorber side, rather than from the window [CdS] side). Our initial experiments have focused on maximizing the collection efficiency of this bottom cell, but future work will focus on non-inverted homojunctions or high-temperature, superstrate heterojunctions such as are currently used in CdTe/CdS solar cells [9].

## GROWTH

A prototype device was grown following the sequence above and Fig. 2. $SnO_2$:F thin films were grown on each side of soda-lime glass by chemical vapor deposition. Next, a 2-μm-thick layer of $CuIn_xGa_{1-x}Se_2$ (x ~0.3) was grown by co-evaporation using a "3-stage" process [10] with a maximum substrate temperature of 605˚C (measured by a thermocouple touching the backside of the substrate) for about 15 minutes. The substrate was then flipped in the holding bracket during a brief exposure to air, and a 2-μm-thick layer of $CuGaSe_2$ was grown by the 3-stage process. The maximum temperature during the $CuGaSe_2$ growth was 610˚C for 10 minutes. P/n junctions were formed simultaneously for both cells during an n-CdS chemical-bath deposition of about 60˚C. Two ZnO layers, one intrinsic and the other conductive ZnO:Al, were grown by RF magnetron sputtering at room temperature onto the CdS layers of each cell. The cells were completed by depositing Al grid contacts onto the ZnO layers.

The growth of each absorber layer during the 3-stage process was monitored by a thermocouple on the back of the substrate. The endpoint of the deposition was clearly detected for both films by a drop in substrate temperature during the end of the second stage of growth. Devices grown in reverse order (CGS first, CIGS last) showed a similar endpoint temperature trend. X-ray diffraction scans showed the films to be phase pure. Figure 3 shows cross-sectional scanning electron microscopy (SEM) images of $CuGaSe_2$ (grown first) and $CuIn_xGa_{1-x}Se_2$ (grown last) films. The images reveal large-grained, dense films with good nucleation to the $SnO_2$ back contact. Electron probe microanalysis

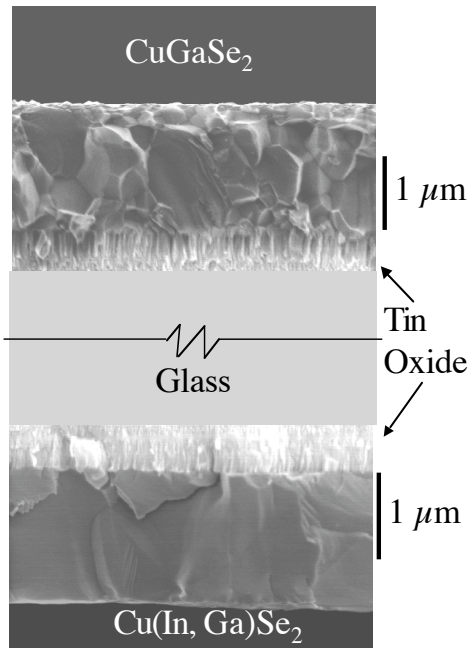


Figure 3. Cross-sectional SEM images of CGS and CIGS films grown on bifacially coated tin oxide glass.

(EPMA) results confirmed composition for each film as expected by deposition rate.

Phase-pure, large-grained films are produced for both films regardless of growth order. However, in limited depositions, the second film grown (either CIGS or CGS) was too conductive to form a rectifying junction with CdS. EPMA results for the film grown second indicate that the film's composition is less than ideal. The thermocouple-monitoring scheme may not be suitable for the second film grown due to the increased thermal resistance of the first-frown film, on which the thermocouple rests. There is some indication from film composition results that the temperature dip lags behind the true substrate temperature and thus does not accurately predict the proper compositional endpoint to the growth. Deposition-rate-determined, timed 3-stage or co-deposition growth should be explored to ensure proper film composition.

## RESULTS

Figure 4 shows current density/voltage (J/V) curves under ~AM1.5 illumination for the first prototype tandem device subcells by probing each cell individually and for "rider" cells that were deposited at the same time as the tandem cells. A schematic diagram of each device, the electrical probe points, and the direction of the incident light is shown to the right of each graph. Table 1 gives open circuit voltage ($V_{oc}$), short circuit current density ($J_{sc}$), fill factor (FF), and efficiency (□) values for each cell shown in Fig. 4.

Figures 4a,c show the device to function as a four-terminal tandem solar cell. The combined efficiency

Table 1. J/V parameters for cells shown in Fig. 4. Cell letters correspond to those in Fig. 4. TO = $SnO_2$

| Cell | Voc (V) | Jsc ($mA/cm^2$) | FF (%) | □ (%) |
|---|---|---|---|---|
| a) CGS/TO | 0.83 | 8.0 | 49.4 | 3.3 |
| b) CGS/Mo | 0.82 | 13.7 | 52.9 | 6.0 |
| c) CIGS/TO | 0.26 | 5.6 | 30.2 | 0.4 |
| d) CIGS/TO | 0.34 | 27.6 | 25.8 | 2.5 |
| e) CIGS/Mo | 0.67 | 33.2 | 74.4 | 16.3 |

of the prototype tandem operating under a common illumination is ~3.7%, with a total $V_{oc}$ of 1.1 V. Fortunately, the tandem device outperforms the more mature CIGS/TO device illuminated through the window layer (4d).

Absolute external quantum efficiencies for the individual tandem cells are shown in Fig. 5. Also shown are QE results for our best cells and for cells grown on Mo back contacts. The collection efficiencies of both the CIGS and CGS cells on $SnO_2$ are approaching those grown on Mo, but the inverted CIGS cell on $SnO_2$ is severely limited.

## DISCUSSION

The top $CuGaSe_2$ cell (Fig. 4a) has good $V_{oc}$, but suffers from low $J_{sc}$ and FF, with an efficiency of 3.3%. A Mo-coated glass substrate "rider" during the $CuGaSe_2$ growth had about twice the efficiency due to a much better fill factor (Fig. 4b). This may indicate that the $CuGaSe_2/SnO_2$ back contact is not ohmic. Figure 4c shows the J/V curves for the $CuIn_xGa_{1-x}Se_2$ bottom cell after the incident light was filtered by the top $CuGaSe_2$ cell. A low collection efficiency, due to the inverted configuration and the non-optimum absorber thickness, accounts for the 0.43% efficiency. This poor collection efficiency is also revealed in the quantum efficiency (QE) data given in Fig. 5. The $CuIn_xGa_{1-x}Se_2$ cell, illuminated from the n-CdS side (Fig. 4d), gave much higher currents, but a poor back contact contributed to the low FF. A Mo-coated, glass substrate "rider" during the $CuIn_xGa_{1-x}Se_2$ growth produced a cell 6.6 times more efficient (Fig. 4e).

The J/V curves of Fig. 4 indicate $SnO_2$ to be a poor back contact to CGS and CIGS, severely limiting the performance of the tandem cells. The shorting junction between a p-type CIGS or CGS film and an n-type TCO film is not ideal due to the inability to highly dope the p-type materials. Other n-type TCO materials have been tested for possible use as a back contact by our group, but secondary ion mass spectroscopy (SIMS) and electron beam-induced current (EBIC) data show $SnO_2$ to be one of the better choices due to its chemical stability and less rectifying contact with CGS. Efforts are under way to use p-type TCOs in place of the more common n-type, which should considerably improve the device performance.

The poor QE values for the inverted bottom cell are due to the high absorption coefficient of the CIGS. Only long-wavelength light is capable of penetrating deep enough into the CIGS to make collectable electron-

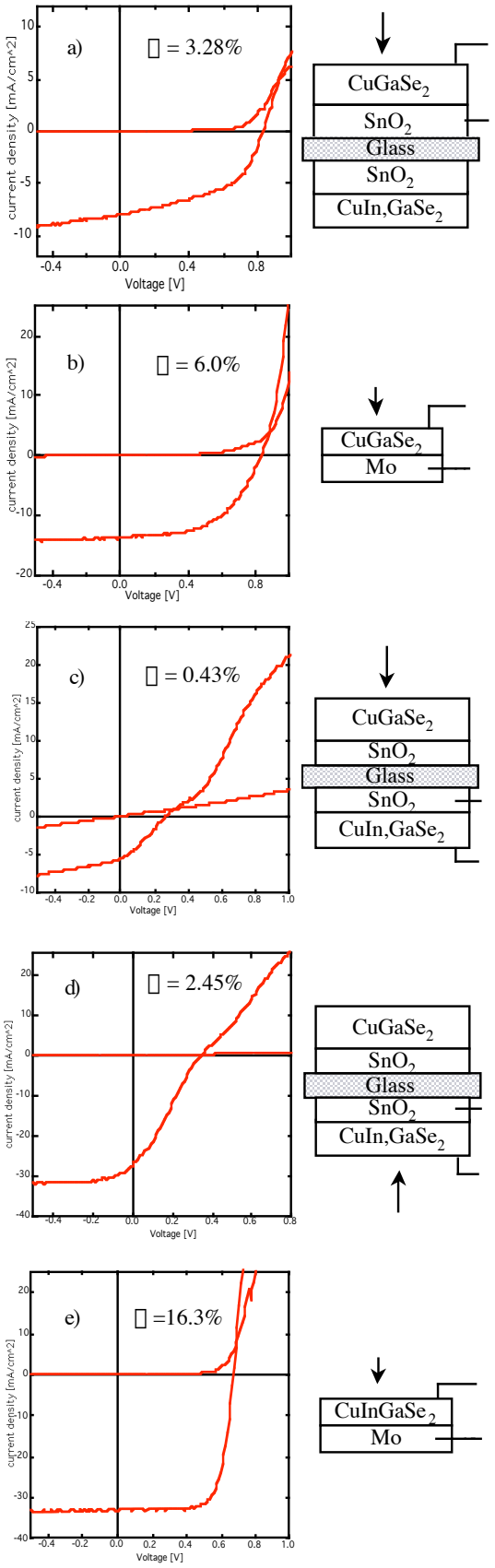


Figure 4. J/V curves for tandem subcells. The CdS and ZnO layers are not shown for clarity.

hole pairs. To enhance this collection efficiency, we grew an Al film in place of grids on a bottom CIGS cell (see Fig. 2) to reflect light back into the collection region. Figure 5 shows the increased QE with the back reflector added to a CIGS bottom cell grown separately. Additional light collection in the bottom cell could be realized by thinning the CIGS absorber layer to move the collection region closer to the back of the absorber

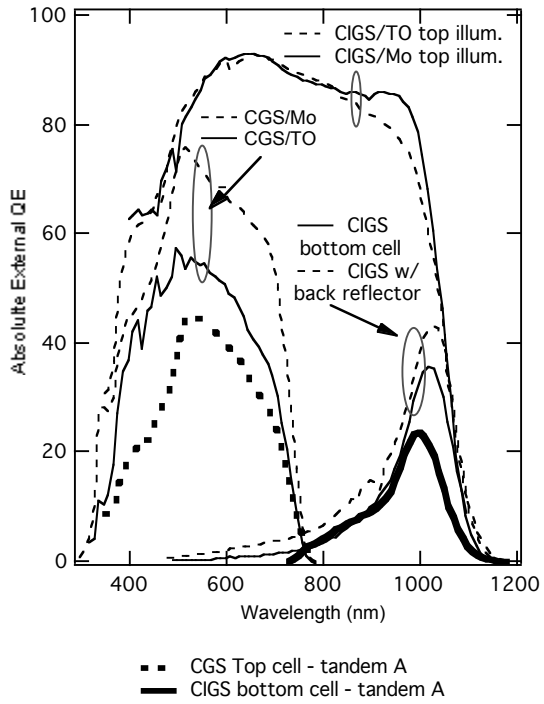


Figure 5. Absolute external quantum efficiencies.

layer and increasing the doping in the CdS layer to increase the depletion width in the CIGS.

Optical absorption in the top CGS cell is great than 97% for above-bandgap light; but unfortunately, it is nearly 20% below the bandgap to ~1200 nm. This non-ideal sub-bandgap absorption limits the current available to the bottom cell. Using high-efficiency QE values for CIGS solar cells and convoluting the CGS sub-bandgap absorption with the AM1.5 spectrum give a theoretical current density of 12.1 mA/cm$^2$ available to a CIGS bottom cell. Again, using high-efficiency $V_{oc}$ and FF values, we calculate a possible bottom-cell efficiency of 6.5%. This implies that only a 12.3%-efficient CGS top cell is needed in the tandem configuration to match current state-of-the-art CIGS cells without further optical improvements in the top cell.

## CONCLUSIONS

Our new non-mechanically stacked, bifacial, four-terminal tandem device allows both cells to be fabricated essentially simultaneously, thus sequencing the high-temperature steps so as to not damage the temperature-sensitive layers. Our initial prototype proved the concept workable, but further research in growth, collection efficiency, and improved back contacts is needed. The single substrate, ease of making contacts, and one high-temperature growth step may make this tandem device design appealing to industry if efficiencies can be boosted above single-junction cell values.

## REFERENCES


[1] T. Takamoto, T. Agui, E. Ikeda, and H. Kurita: "High efficiency InGaP/$In_{0.01}Ga_{0.99}As$ tandem solar cells lattice-matched to Ge substrates," Solar Energy Materials and Solar Cells **66**, 2001, pp. 511-516.

[2] S. Okamoto, E. Maruyama, A. Terakawa, W. Shinohara, S. Nakano, Y. Hishikawa, K. Wakisaka, and S. Kiyama: "Towards large-area, high-efficiency a-Si/a-SiGe tandem solar cells," Solar Energy Materials and Solar Cells **66**, 2001, pp. 85-94.

[3] T. J. Coutts, K. A. Emery, and J. S. Ward: "Modeled performance of polycrystalline thin-film mulijunction solar cells," Progress in Photovoltaics and Applications **10**, 2002, pp. 1-9.

[4] M. A. Contreras, B. Egaas, K. Ramanathan, J. Hiltner, A. Swartzlander, F. Hasoon, and R. Noufi: "Progress toward 20% efficiency in Cu(In,Ga)$Se_2$ polycrystalline thin-film solar cells," Progress in Photovoltaics and Applications **7**, 1999, pp. 311-316.

[5] V. Nadenau, D. Hariskos, and H. W. Schock, Proceedings of the 14th European Photovoltaic Solar Energy Conference. Stephens & Assoc., Bedford, U.K., 1997, p. 1250.

[6] M. Saad, H. Riazi, E. Bucher, and M. C. Lux-Steiner: "$CuGaSe_2$ solar cells with 9.7% power conversion efficiency," Applied Physics A **62**, 1996, pp. 181-185.

[7] P. Gashin, A. Focsha, T. Potlog, A. V. Simashkevich, and V. Leondar: "n-ZnSe/p-ZnTe/n-CdSe tandem solar cell," Solar Energy Materials and Solar Cells **46**, 1997, pp. 323-331.

[8] D. L. Morel: "Progress on high efficiency thin film solar cells," Solar Cells **24**, 1988, pp. 157-164.

[9] X. Wu, R. Ribelin, R. G. Dhere, D. S. Albin, T. A. Gessert, S. Asher, D. H. Levi, A. Mason, H. R. Moutinho, and P. Sheldon: "High-efficiency $Cd_2SnO_4/Zn_2SnO_4/Zn_xCd_{1-x}S$/CdS/CdTe polycrystalline thin-film solar cells," Proceedings of the 28th IEEE Photovoltaic Specialists Conference, 2000, pp. 470-474.

[10] NREL: "U.S. Patent No. 5,436,204," (1995).

# REPORT DOCUMENTATION PAGE

*Form Approved*
*OMB NO. 0704-0188*



| 1. AGENCY USE ONLY (Leave blank) | 2. REPORT DATE | 3. REPORT TYPE AND DATES COVERED |
|---|---|---|
| | May 2002 | 29th IEEE PVSC-Conference Paper<br>May 20-24 2002 |

**4. TITLE AND SUBTITLE**
A New Thin-Film $CuGaSe_2$/Cu(In,Ga)$Se_2$ Bifacial, Tandem Solar Cell With Both Junctions Formed Simultaneously: Preprint

**5. FUNDING NUMBERS**
PVP14901

**6. Author(S)**
D. L. Young, J. Abushama, R Noufi, X. Li, J. Keane, T. A. Gessert, J. S. Ward, M. Contreras, M. Symko-Davies, and T. J. Coutts

**7. PERFORMING ORGANIZATION NAME(S) AND ADDRESS(ES)**
National Renewable Energy Laboratory
1617 Cole Blvd.
Golden, CO 80401-3393

**8. PERFORMING ORGANIZATION REPORT NUMBER**

**9. SPONSORING/MONITORING AGENCY NAME(S) AND ADDRESS(ES)**
National Renewable Energy Laboratory
1617 Cole Blvd.
Golden, CO 80401-3393

**10. SPONSORING/MONITORING AGENCY REPORT NUMBER**
NREL/CP-520-31440

**11. SUPPLEMENTARY NOTES**

**12a. DISTRIBUTION/AVAILABILITY STATEMENT**
National Technical Information Service
U.S. Department of Commerce
5285 Port Royal Road
Springfield, VA 22161

**12b. DISTRIBUTION CODE**

**13. ABSTRACT** *(Maximum 200 words)*:
Thin films of $CuGaSe_2$ and Cu(In,Ga)$Se_2$ were evaporated by the 3-stage process onto opposite sides of a single piece of soda-lime glass, coated bifacially with an n +/-TCO. Junctions were formed simultaneously with each of the p-type absorbers by depositing thin films of n-CdS via chemical bath deposition (CBD) at 60°C. The resulting four-terminal device is a non-mechanically stacked, two-junction tandem. The unique growth sequence protects the temperature-sensitive p/n junctions. The initial device (h = 3.7%, $V_{oc}$ = 1.1 V [AM1.5]) suffered from low quantum efficiencies. Initial results are also presented from experiments with variations in growth sequence and back reflectors.

**14. SUBJECT TERMS:** PV; tandem solar cell; thin-film; three-stage process; four-terminal device; scanning electron microscopy (SEM); electron probe microanalysis (EPMA); high-temperature-sensitive layers;

**15. NUMBER OF PAGES**

**16. PRICE CODE**

| 17. SECURITY CLASSIFICATION OF REPORT | 18. SECURITY CLASSIFICATION OF THIS PAGE | 19. SECURITY CLASSIFICATION OF ABSTRACT | 20. LIMITATION OF ABSTRACT |
|---|---|---|---|
| Unclassified | Unclassified | Unclassified | UL |

NSN 7540-01-280-5500

Standard Form 298 (Rev. 2-89)
Prescribed by ANSI Std. Z39-18
298-102